

- (pps)]PF₆ (M = Co, Ni) complexes.¹³
- (17) L. Sacconi and R. Morassi, *J. Chem. Soc. A*, 2997 (1968); L. Sacconi, I. Bertini, and F. Mani, *Inorg. Chem.*, **7**, 1417 (1968).
- (18) P. W. R. Corfield, R. J. Doedens, and J. A. Ibers, *Inorg. Chem.*, **6**, 197 (1967).
- (19) D. T. Cromer and J. A. Waber, *Acta Crystallogr.*, **18**, 104 (1965).
- (20) R. F. Stewart, E. R. Davidson, and W. T. Simpson, *J. Chem. Phys.*, **42**, 3175 (1965).
- (21) D. T. Cromer, *Acta Crystallogr.*, **18**, 17 (1965).
- (22) Owing to the proximity of the special position $\bar{3}$ there is no room to accommodate more than one molecule of acetone; therefore the carbon atom (AC) and the oxygen atom (AO) were allotted population parameters of 0.5 and 0.167, respectively.
- (23) D. D. Titus, A. A. Orio, R. E. Marsh, and H. B. Gray, *Chem. Commun.*, 322 (1971).
- (24) A. Orlandini and L. Sacconi, *Cryst. Struct. Commun.*, **4**, 107 (1975).
- (25) H. D. Kaesz and R. B. Saillant, *Chem. Rev.*, **72**, 231 (1972).
- (26) L. Sacconi, *J. Chem. Soc. A*, 248 (1970).

Contribution from the Department of Chemistry and Materials Research Center, Northwestern University, Evanston, Illinois 60201, and Philips Laboratories, Briarcliff Manor, New York 10510

Single-Crystal Raman Evidence for and X-Ray Analysis of the Distorted Square-Pyramidal Pentachlorothallate and Pentachloroindate Complexes in [(C₂H₅)₄N]₂[TiCl₅] and [(C₂H₅)₄N]₂[InCl₅]

G. JOY, A. P. GAUGHAN, Jr., I. WHARF, D. F. SHRIVER,* and J. P. DOUGHERTY

Received March 25, 1975

AIC502063

Detailed single-crystal vibrational data and X-ray space group determinations reveal that the tetraethylammonium salts of InCl₅²⁻ and TiCl₅²⁻ are isomorphous and isostructural. High-quality single-crystal Raman data were collected on well-formed crystals with polished faces. This new data in conjunction with low-temperature infrared and Raman spectroscopy had led to a major reinterpretation of the previous vibrational assignments for [(C₂H₅)₄N]₂[InCl₅] and in the process clarified an ambiguity in the previous vibrational work. The new assignments, which indicate that the InCl₅²⁻ ion does not have full C₄ symmetry, and second harmonic generation experiments, which indicate that the crystal may not be centrosymmetric, prompted reassessment of the published X-ray data. An alternate refinement is presented which is based on C₂ symmetry for the InCl₅²⁻ ion.

Introduction

Although many five-coordinate complexes are known among the main-group elements, only two systems having monodentate ligands and lacking lone electron pairs on the central atom have been shown to have square-pyramidal structures by X-ray diffraction studies. These are (C₆H₅)₅Sb¹ and InCl₅²⁻ in the salt [(C₂H₅)₄N]₂[InCl₅],² the last of which has been studied in greater detail because of its simplicity and reported rigorous fourfold symmetry. The general motivation for structural and vibrational work on these systems is the lack of a ready explanation of their geometry and the implication of the square-pyramidal configuration in the Berry pseudorotation mechanism for the stereochemical nonrigidity of trigonal-bipyramidal compounds.³

In addition to the crystal structure determination, InCl₅²⁻ has been investigated in solution,^{4,5} various salts have been prepared,⁵⁻⁷ and two single-crystal vibrational studies have appeared,^{8,9} which form the basis of normal-coordinate vibrational analyses.^{3,10} In both papers on the single-crystal spectra, one more E symmetry vibration was observed than would be expected for a square-pyramidal C₄ symmetry InCl₅²⁻ ion, and, for want of a better assignment, this extra vibration was attributed to a lattice mode.^{8,9}

We undertook the present work on [(C₂H₅)₄N]₂[TiCl₅] in the hope that the results might help to clarify the ambiguities in the InCl₅²⁻ vibrational data. In addition, we sought a positive test of the contention that the indium and thallium salts are isostructural.⁵ The results led us to question the rigorous C₄ symmetry previously assigned to these complexes and therefore prompted a reinvestigation of the [(C₂H₅)₄N]₂[InCl₅] X-ray structure.

Experimental Section

[(C₂H₅)₄N]₂[TiCl₅] and [(C₂H₅)₄N]₂[InCl₅] were prepared by the published methods⁵ and crystallized from acetonitrile—containing

* To whom correspondence should be addressed at Northwestern University.

a 50% excess of (C₂H₅)₄NCl—by slow evaporation of the solvent at room temperature. The crystals used for vibrational data collection had polished perpendicular faces, ca. 3 × 3 × 1.5 mm on a side, and were oriented by the aid of a polarizing microscope and their morphology.

Raman spectra were obtained on a 0.85-m Spex 1401 double monochromator with sampling optics of our own design and extensively modified Spex photon-counting electronics. A 1-cm⁻¹ band pass was employed in all experiments. Data on the single crystals were collected on magnetic tape at 0.17-cm⁻¹ intervals and were processed on the CDC 6400 computer by the program RAMAN.¹¹ Among its various functions, RAMAN allows least-squares fitting of component bands via a modified version of the Pitha and Jones routine.¹² The 647.1-nm line of a light-feedback-stabilized Kr-ion laser (Spectra Physics 164) was used for sample illumination. Laser power, ca. 100 mW, was measured at the sample and was readjusted to a fixed value for both orientations of the incident electric vector. Plasma lines were removed by a premonochromator in the laser beam, and peak positions were accurately located relative to Ne atomic lines, introduced by a Ne bulb close to the sample.

For low-temperature runs, a cylindrical laser focusing lens (*f* = 90 mm) was used to minimize local heating and an oblique (ca. 160°) back-scattering geometry was employed. The polycrystalline sample in the form of a pressed disk was attached to a copper block by Eccotherm TC-4 (Emerson and Cummings, Northbrook, Ill.) and cooled by a transfer gas in a double-chamber helium dewar. Temperature of the sample was monitored by a Au-Fe vs. Cu thermocouple attached to the side of the sample by Eccotherm. The absolute temperatures are estimated to be known to ±4° and relative temperatures are ±2°. Peak positions were measured relative to the exciting line, 647.089 nm, and two Kr-plasma lines, 651.095 and 657.007 nm.

Infrared spectra of Nujol mulls between polyethylene plates were obtained using a Perkin-Elmer 180 far-infrared spectrometer which was calibrated using water vapor lines and is accurate to ±1 cm⁻¹; however, the breadth of the infrared bands leads to a greater uncertainty than this.

Precession, Laue, and Weissenberg photographs taken with both Mo and Cu radiation were employed to assign the Laue class, lattice type, and apparent space group. Lattice constants at 22° were

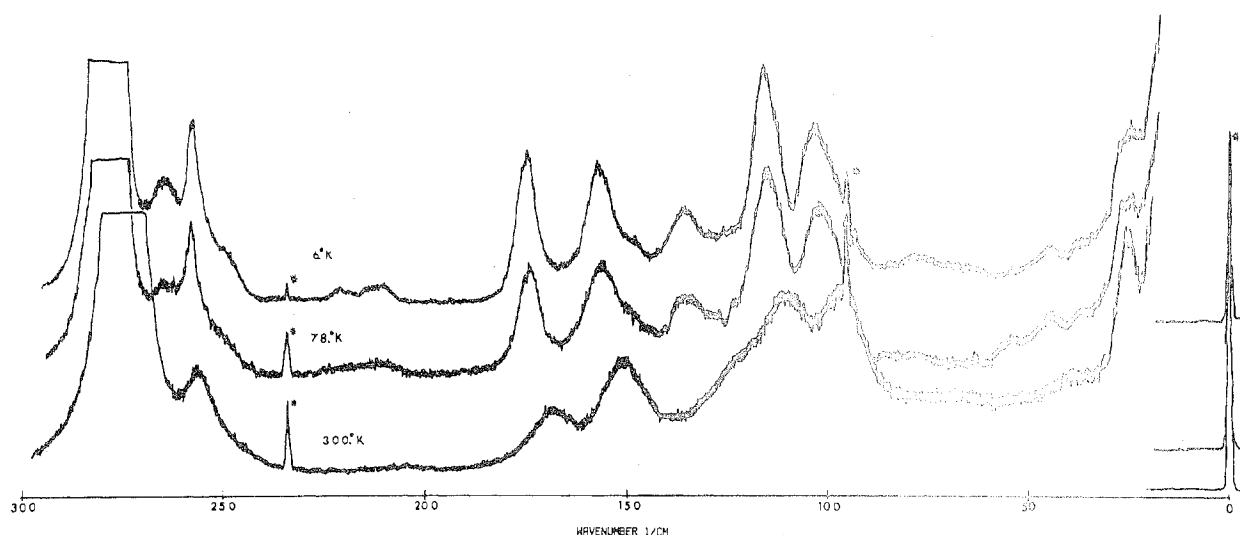


Figure 1. Variable-temperature Raman spectra of polycrystalline $[(C_2H_5)_4N]_2[TiCl_5]$. The greatly attenuated 6471-Å laser line and plasma lines are indicated by asterisks.

obtained from zero-level precession photographs. A single crystal of the In complex, ca. $0.40 \times 0.40 \times 0.50$ mm, was mounted on the diffractometer with the [110] direction approximately coincident with the spindle axis. This crystal was in the form of a well-developed truncated octahedron with faces belonging to the forms {100}, {101}, and {001}. The mosaic spread, 0.5° , at half-height, which was determined by narrow-source ω scans on several strong reflections, is acceptably low. Lattice constants were determined from least-squares refinement¹⁷ of setting angles for 12 reflections using Mo $K\alpha$ radiation (λ 0.70930 Å) at a takeoff angle of 1.5° and agreed to within 0.25% with those of Brown, Einstein, and Tuck.² Intensity data for reflections in the $hk0$ zone were collected by the θ - 2θ scan technique on a computer-controlled Picker FACS-1 automatic diffractometer, with the pulse height analyzer set to accept approximately 90% of the Mo $K\alpha$ line. In a test for possible phase changes, X-ray powder diffraction data were collected in both energy and wavelength dispersive modes at room temperature and 77°K. Copper $K\alpha$ radiation was employed and the diffractometer scan ranged between 10 and 50° in 2θ .

A second harmonic generation (SHG) test¹³ was used to provide a center of symmetry determination.¹⁴ The experiment was performed with a second harmonic analyzer¹⁵ which produces and analyzes SHG in test crystals while determining if the radiation produced is true SHG through a detector assembly designed to function as a single-wavelength (λ 5300 Å) spectrometer. SHG signals at a level $1/1000$ of that produced in a crystalline quartz (α -SiO₂) standard can be reliably detected over a dynamic range of 50 db. At this level of sensitivity, it is possible to establish center of symmetry determination with >99% reliability.¹⁶

Results and Discussion

Low-Temperature Spectra for $[(C_2H_5)_4N]_2[TiCl_5]$. Variable-temperature Raman spectra were obtained on a polycrystalline sample at 6, 14, 33, 78, and 300°K. The results at three of these temperatures are summarized in Figure 1, which shows the expected sharpening of the bands and their shift to higher frequency. Of particular importance is the resolution of several distinct features at 6°K which are either barely evident or absent at higher temperatures and which form the basis for deconvolution of the room-temperature single-crystal data. Another useful aspect of the low-temperature data was the observation that normalized temperature coefficients for peak positions are significantly larger for E modes than for either A or B modes. These temperature coefficients, χ , were calculated between 300 and 6°K via¹⁸

$$\chi = \frac{\nu_{300} - \nu_6}{(300 - 6)\nu_{av}}$$

where ν_n represents the peak position in cm^{-1} at temperature n .

It is important to the interpretation that no phase changes occur over the temperature range studied. The spectral data provide a strong indication that this condition is met, as there are no abrupt or radical changes in the spectra for either the internal or the lattice mode region. Furthermore, no soft lattice modes, with characteristic high-temperature coefficients were observed. Low-temperature (77°K) powder diffraction data revealed a small shrinkage in all lattice parameters from their room-temperature values. Again the indication is that no phase change occurs in the temperature range of importance in the low-temperature spectroscopic measurements.

Selection Rules. The only systematic absences which can be established with certainty from the precession and Weissenberg photographs ($h00, k \neq 2n$) indicate that the space group is $P4/n$. Unit cell constants ($a = 9.35$ (2) and $c = 14.10$ (2) Å for the indium salt; $a = 9.37$ (2) and $c = 14.06$ (2) Å for the thallium salt) along with the measured densities demonstrate two molecules per unit cell (for In, $d_{obsd} = 1.46$ (3), $d_{calcd} = 1.48$ g/cm³; for Tl, $d_{obsd} = 1.71$ (3), $d_{calcd} = 1.73$ g/cm³). These findings agree with the results of Brown, Einstein, and Tuck for the indium salt² and establish that the two salts are in fact isomorphous. The close similarity of intensity patterns for the $hk0$ zones for the two salts carries through to their single-crystal vibrational spectra, leaving no doubt that they are strictly isostructural.

As will be described below, careful analysis of the vibrational data reveals that the MX_5^{2-} species do not possess the full fourfold site symmetry required by their positions in $P4/n$. Therefore, to keep the discussion general, it is necessary at this point to consider all of the tetragonal subgroups of the Laue class $4/m$, for which selection rules are given in Table I assuming two formula units per unit cell.

Assignments for $TiCl_5^{2-}$. The correlation diagrams of Table I result in two possible patterns for the factor group splitting: (1) 18 Raman-active frequencies with coincidences in the Raman and infrared spectra— C_4 and S_4 unit cells or (2) 9 Raman bands lacking coincidence with 9 other infrared frequencies— C_{4h} unit cell. Contrary to these unit cell selection rules, inspection of Table II reveals 14 bands in the internal mode region (274 – 95 cm^{-1}) of the $TiCl_5^{2-}$ Raman spectrum, and as will be described later, the correspondence between infrared and Raman features is almost within experimental error. The disparity between experiment and selection rules for the factor groups is even more striking if two of the observed bands are attributed to the cation owing to their coincidence in frequency, shape, and intensity with two features in the

Table I

Correlation of the MX₅ Vibrational Symmetry Species for Alternative Site Symmetries with Those of an S₄ Unit Cell

C _{4v} ion ^a	C ₄ ion ^b	C ₂ site ^c	S ₄ unit cell (Z = 2)
3 A ₁	3 A	6 A	6 A
2 B ₁	3 B	6 B	6 B
1 B ₂			
3 E	3 E	6 B	6 E

Correlation of the Selection Rules for Various Possible Unit Cells (Z = 2)

S ₄	C _{4h}	C ₄
6 A (xx + yy, zz)	3 A _g (xx + yy, zz)	6 A (xx + yy, zz)(z)
6 B (xx - yy, xy)(z)	3 B _g (xx - yy, xy)	6 B (xx - yy, xy)
	3 E _g (xz, yz)	
6 E (xz, yz)(x, y)	3 A _u (z)	6 E (xz, yz)(x, y)
	3 B _u (silent)	
	3 E _u (x, y)	

^a For the free C_{4v} ion: stretches = 2 A₁ + B₁ + E, deformations = A₁ + B₁ + B₂ + 2 E. ^b For the C₄ symmetry ion: stretches = 2 A + B + E, deformations = A + 2 B + 2 E. ^c For the C₂ symmetry ion: stretches = 3 A + 2 B, deformations = 3 A + 4 B.

[(C₂H₅)₄N]₂[InCl₅] spectrum. The remaining 12 active fundamentals with coincident infrared frequencies are the same as predicted for C₂ (or lower) site symmetry, and it follows that correlation field splitting is negligible.

Even though the spectra are interpreted in terms of C₂ site symmetry, selection rules for the vibrations follow unit cell transformation properties. The ensuing discussion is based on transformation properties and symmetry species of the S₄ unit cell, but as may be determined from Table I a similar interpretation results for the C₄ unit cell. In an S₄ unit cell assignment with negligible factor group coupling, the 6 A modes of the C₂ symmetry MX₅ complex transform as 3 A

and 3 B crystal modes, and the 6 B modes of the C₂ MX₅²⁻ complex transform as 6 E crystal modes. An ordered structure in the C_{4h} unit cell would require fewer than the observed number of bands.¹⁹

The data of Table II fall into three logical regions: stretching modes between 275 and 200 cm⁻¹, deformations between 170 and 95 cm⁻¹; and lattice modes below 80 cm⁻¹. It is convenient to consider first the specific assignment of A and B modes and then the more complex E assignments.

With the exception of the B mode, the assignments are obvious from casual inspection of the single-crystal spectra in the Ti-Cl stretching region, Figure 2. Careful inspection of the intensities indicates the missing B mode lies under the 273-cm⁻¹ A feature. While some leakage into the z(y, x)y spectrum (where B should be active) by the very intense A mode is expected, there is much higher relative intensity, 54, in this orientation, than found for z(x, z)y, 15, where the B mode should be absent. The lack of correlation field splitting is evident in the stretching region where 2 A, 1 B, and 2 E Raman frequencies are observed.

Assignment of the A and B deformations is completely straightforward from the single-crystal spectra. As expected the A mode at 118 cm⁻¹ has no counterpart in the infrared spectrum. Two B modes are found in the Raman spectrum at 168 and 150 cm⁻¹ and are absent in the infrared spectrum as required by the selection rules.

The low-temperature Raman spectra are an important supplement to the single-crystal data in assigning the E modes. At 6°K two additional features are clearly evident in the stretching region, one as a maximum at 264 cm⁻¹ and the other as a distinct shoulder at 251 cm⁻¹. These two features have normalized temperature coefficients of -12 (2) × 10⁻⁵ and -10 (4) × 10⁻⁵ deg⁻¹, respectively, between 300 and 6°K, which contrast with the temperature coefficients of -7 (1) × 10⁻⁵ and -3 (1) × 10⁻⁵ deg⁻¹ for the two strong bands at 273 and 255 cm⁻¹ associated with nondegenerate representations. In agreement with the low-temperature data the room-temperature z(x, z)y spectrum, Figure 2, contains a highly asymmetric E feature with a maximum at 256 cm⁻¹. Least-squares resolution of this feature into two components (Figure 2) reveals the presence of one band at 256.2 cm⁻¹ and

Table II. Single-Crystal Raman Data for [(C₂H₅)₄N]₂[TiCl₅] Orientations and Corresponding Observed Intensities^a

Symmetry ^b	Freq ^c	Intensity							
		z(x, x)y	z(y, x)y	z(x, z)y	z(y, z)y	y(z, z)x	y(x, y)x	y(x, z)x	y(z, y)x
B	273.7 (2)	958	54	15 ^d	31	403	131	30	30
A	273.3 (2)			14 ^d	12				
E	256.2 (3)	46	4	14 ^d	12	70	8	15	18
A	255.2 (1)			6 ^d	5				
E	244.8 (10)	3	2	3 ^d	2	80	1	2	1
A ^{?e}	205.5 (20)								
B ^e	203.0 (20)	4	66	3 ^d	2	41	80	2	1
B	167.7 (2)			2	2				
B	150.3 (4)	135	28	3 ^d	2	41	41	2	1
E	136.2 ^d (-)			12 ^d	12				
E	125.2 (2)	18	2	25 ^d	24	94	30	30	35
A	118.2 (3)			81	86				
E	109.8 (3)	34	12	94 ^d	81	10	6	94	107
E	96.1 (3)			100 ^d	86				
B ^f	78.3 (10)	4	12	3 ^d	16	3	10	17	22
E ^f	66.4 (10)			14 ^d	16				
E ^f	52.9 (20)	2	31	11 ^d	10	8	13	13	17
B ^f	41.1 (2)			7	15				
E ^f	26.1 (2)	4	2	34 ^d	33	7	4	39	45
E ^f	26.1 (2)			4	4				

^a Within each set z(. . .)y, z(. . .)x, and y(. . .)x intensities of the resolved component bands are normalized with respect to the intensity of the 96.1-cm⁻¹ band in the . . . (x, z) . . . orientation. For the sake of brevity, results for the four possible z(. . .)x orientations are omitted. These results agree with those presented. ^b Vibrational species for the S₄ unit cell. ^c Frequencies in cm⁻¹ are an average of all spectra scanned and have an estimated absolute accuracy of 0.5 cm⁻¹. Standard deviations in the last digits are given in parentheses. ^d Frequencies and intensities resulting from digital least-squares fitting. ^e These weak features are found in the same positions in [(C₂H₅)₄N]₂[InCl₅] and are therefore associated with the [(C₂H₅)₄N]⁺ cation. ^f Lattice modes.

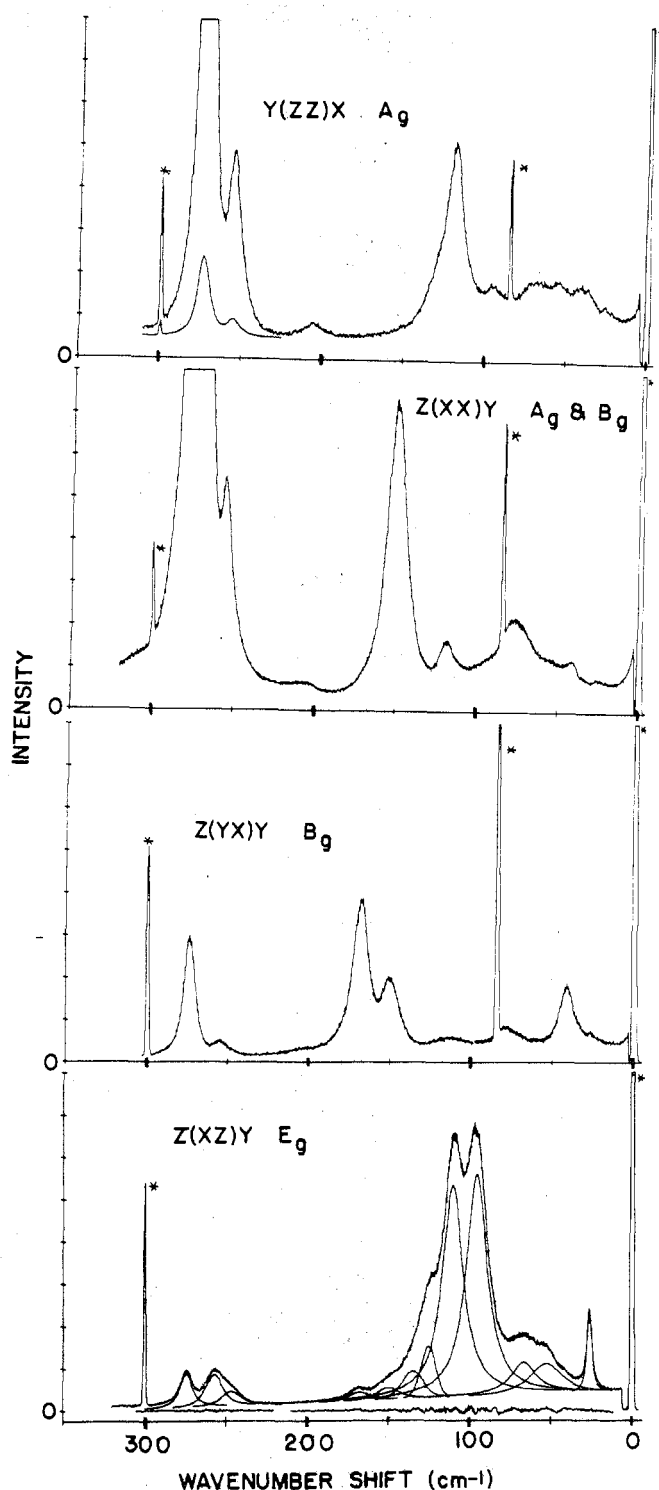


Figure 2. Single-crystal Raman spectra. The lowest spectrum includes the computer-resolved components and the difference between the observed spectrum and the composite of the calculated components.

a weaker one at 244.8 cm^{-1} . The 12- cm^{-1} separation of these components conforms to the 13- cm^{-1} separation observed in the 6°K spectrum. The low-temperature infrared spectrum is characterized by shifts of maxima to higher frequencies by 4–8 cm^{-1} . The stretch region has a medium peak at 276 cm^{-1} and a broad, strong peak at 252 cm^{-1} , which correspond with bands in the low-temperature Raman spectrum at 278 and 251 cm^{-1} .

The E deformation assignments follow a similar pattern. At 6°K a distinct shoulder occurs at 148 cm^{-1} and maxima

are found at 135, 116, and 104 cm^{-1} in addition to those features previously mentioned for the B modes. The frequency-normalized temperature coefficients are $-38 (2) \times 10^{-5}$, $-34 (2) \times 10^{-5}$, $-22 (2) \times 10^{-5}$, and $-29 (2) \times 10^{-5} \text{ cm}^{-1} \text{ deg}^{-1}$, respectively, which contrast with the smaller magnitude of temperature coefficients for nondegenerate modes which range between $-15 (1) \times 10^{-5}$ and $-17 (1) \times 10^{-5} \text{ cm}^{-1} \text{ deg}^{-1}$. The least-squares resolution of the room-temperature single-crystal $z(x, z)y$ spectrum was accomplished in two steps. Initially, the deconvolution was performed by assuming three distinct E internal modes at 125, 110, and 96 cm^{-1} as well as three E lattice modes at 66, 52, and 26 cm^{-1} . In addition, two components were introduced for the 168- and 150- cm^{-1} B modes which show a small amount of leakage into this spectrum. With the exception of the 136- cm^{-1} region a good fit was obtained. In a second deconvolution an additional feature was introduced at 137 cm^{-1} which refined to 136 cm^{-1} to give an excellent fit. The 11- cm^{-1} separation of the 136- and 125- cm^{-1} features in the resolved $z(x, z)y$ spectrum agrees well with the 13- cm^{-1} separation observed at 6°K. The low-temperature infrared spectrum is composed of weak bands at 145, 130, and 102 cm^{-1} which correspond with the 148-, 135-, and 104- cm^{-1} Raman bands, and strong features at 126 and 116 cm^{-1} which correspond to the unresolved 116- cm^{-1} Raman band of a polycrystalline sample at low temperature.

Assignments for InCl_5^{2-} . Between 18 and 210 cm^{-1} the Raman spectrum of polycrystalline $[(\text{C}_2\text{H}_5)_4\text{N}]_2[\text{InCl}_5]$, at 6°K, reveals two peaks at 148 and 133 cm^{-1} not found at room temperature, and these features also are discernible as high as 78°K. New single-crystal data of higher quality than heretofore available are presented in Table III. Deconvolution of the single-crystal data was again performed with the aid of the low temperature data, revealing 11 InCl_5^{2-} bands between 300 and 100 cm^{-1} . Two overlapping A stretches are clearly evident at 292 and 286 cm^{-1} , but no B stretch is apparent. The two E symmetry stretches expected for the anion of a C_2 site, but not for a C_4 site, are evident at 281 and 271 cm^{-1} . Only the latter has been reported in the literature.^{8,9} The B deformation assignments at 191 and 163 cm^{-1} as well as the A assignment at 140 cm^{-1} are straightforward. With the aid of low-temperature data, the four E modes predicted for InCl_5^{2-} at C_2 sites are found at 144, 136, 122, and 103 cm^{-1} in the single-crystal data. With this reinterpretation of the spectrum it is no longer necessary to assume arbitrarily the presence of a lattice mode in this region.^{8,9}

In summary, the vibrational data for the tetraethylammonium salts of InCl_5^{2-} and TlCl_5^{2-} indicate that these complexes reside on sites lacking full C_4 symmetry. The most straightforward conclusion from the vibrational data is that the InCl_5^{2-} ions have local C_2 symmetry, which would be inconsistent with the previous structure determination.² It is conceivable that the space group chosen by Brown, Einstein, and Tuck is correct and the InCl_5^{2-} ions of C_2 local symmetry are disordered around the crystallographic fourfold axis from one InCl_5^{2-} site to the next. Alternatively the InCl_5^{2-} ions may have full C_4 site symmetry but experience a C_2 perturbation of their vibrational modes owing to the local C_2 environment provided by static disordered tetraethylammonium arrays. This latter possibility seemed unlikely to us because the six E symmetry crystal modes, which demonstrate the C_2 distortion are well separated. These considerations led us to inspect alternate interpretations of the crystallographic data.

Reevaluation of the X-Ray Results. The structure of $[(\text{C}_2\text{H}_5)_4\text{N}]_2[\text{InCl}_5]$, as previously reported,² consisted of centrosymmetrically related InCl_5^{2-} ions situated about the Wyckoff c positions of C_4 symmetry in space group $\text{C}_{4h}^3\text{-P4}/n$. Coaxial with the InCl_5^{2-} ions are disordered $(\text{C}_2\text{H}_5)_4\text{N}^+$ ions also situated about the Wyckoff c positions. The N atoms of

Table III. Single-Crystal Raman Data for [(C₂H₅)₄N]₂[InCl₅]^a

Species for S ₄ unit cell	Freq ^b	Intensity						
		y(z, z)x	y(x, y)x	y(z, y)x	y(x, z)x	z(y, y)x	z(x, y)x	z(y, z)x
A	292.0 (2)	395.8	21.8	34.3	23.8	418.1	54.8	23.8
A	285.5 (15)	92.4	20.1	11.3	21.0	306.4	49.1	22.7
E	280.6 (30)			10.0	7.6			5.5
E	270.9 (11)			4.4	5.4			5.0
B ^c	209.3 (15)		4.4			7.1		
A ^c	203.9 (25)	6.1						
B	191.2 (1)		69.8	2.5	7.8	15.8	65.4	4.1
B	171.0 (25)		3.0					
B	163.4 (2)		109.8	4.4	11.0	89.4	92.9	10.5
E	144.3 (26)			18.6	14.5			13.5
A	139.7 (15)	70.6				15.1		
E	136.3 (10)			12.5	10.3			14.0
E	121.6 (1)	21.8	23.0	96.8	104.4	24.5	18.8	103.4
E	103.3 (1)	27.0	17.4	100.0	102.9	22.2	12.2	100.0
B	74.4 (20)					47.2	10.6	
A	69.0 (15)	31.0						
E	68.8 (5)			18.6	31.4			24.5
E	55.1 (13)			36.8	35.0			32.8
A	41.0 (10)	33.1						
B	39.1 (5)		29.9			17.4	32.3	
E	28.8 (5)	15.0	5.0	42.4	50.0	5.3		43.8

^a Within each set z(. . .)x and y(. . .)x intensities of the resolved component bands are normalized with respect to the intensity of the 103.3 cm⁻¹ band in the ... (z, y) ... orientation. ^b Frequencies, in cm⁻¹, are an average of all spectra scanned and have an estimated absolute accuracy of 0.5 cm⁻¹. Standard deviations in the last digit(s) are given in parentheses. ^c These weak features are found in the same positions in [(C₂H₅)₄N]₂[TiCl₅] and are therefore associated with the (C₂H₅)₄N⁺ cation.

the two remaining (C₂H₅)₄N⁺ ions in the unit cell occupy the centrosymmetrically related Wyckoff b sites of S₄ symmetry, the cation as a whole again being disordered. There are two disturbing features of this solution and its subsequent refinement: the disorder of the (C₂H₅)₄N⁺ ions and the significant residual electron density in the region of the basal Cl atoms of the tetragonal-pyramidal anion. The disorder of each of the two distinct types of (C₂H₅)₄N⁺ ions in the unit cell is enforced by their placement relative to the symmetry elements of P4/n. The cations which are coaxial with the InCl₅²⁻ ions are disordered by virtue of the C₄ symmetry axis to which they are constrained. Since the vibrational data suggest a twofold axis for the InCl₅²⁻ ion and, hence, for the coaxial (C₂H₅)₄N⁺ ion as well, an ordered model with crystallographically imposed C₂ rather than C₄ symmetry would be more satisfying. The two remaining (C₂H₅)₄N⁺ ions in the unit cell of the original model are disordered although this disorder is necessitated by the center of symmetry in the previously assigned unit cell and not by their site symmetry (S₄). Thus, an additional feature of the alternative model is the absence of a center of symmetry. This results in crystallographically independent S₄ sites for these two (C₂H₅)₄N⁺ ions.

The significant residual electron density in the region of the basal Cl atoms of the tetragonal-pyramidal anion² might be attributed to one of several effects.²⁰ However, in the present case the residuals are found precisely where the difference between C₂ and C₄ symmetry for the InCl₅²⁻ ion would be expected to manifest itself and therefore suggest an ordered C₂ model for the InCl₅²⁻ ion.

Table IV shows the correlation of allowed point symmetries for the InCl₅²⁻ and (C₂H₅)₄N⁺ ions with the available site symmetries in the Laue class. Within Laue class 4/m there are 14 space groups. The diffraction evidence for a primitive lattice eliminates five of these. Since Z = 2, an acceptable space group must possess C₂ axes of order 2 to accommodate the coaxial InCl₅²⁻ and (C₂H₅)₄N⁺ ions. This condition eliminates all of the remaining space groups based on the point group C_{4h} and also eliminates P4₁ and P4₃. Of the three remaining space groups, P4₂ and P4 do not possess the requisite S₄ sites for the two remaining (C₂H₅)₄N⁺ ions. This leaves S4-P4 as the only space group having the desired combination

Table IV. Correlation of Allowed Point Symmetries for the InCl₅²⁻ and (C₂H₅)₄N⁺ Ions with the Available Site Symmetries in Laue Class 4/m

InCl ₅ ²⁻	(C ₂ H ₅) ₄ N ⁺
4mm (C _{4v}) ^a	4/m (C _{4h})
4 (C ₄) ^c	4 (S ₄) ^b
mm2 (C _{2v})	4 (C ₂) ^c
m (C ₂)	2/m (C _{2h})
2 (C ₂)	m (C ₂)
1 (C ₁)	2 (C ₂)
	1 (C ₁)
	-1 (C ₁)

^a Highest possible point symmetry assuming a tetragonal-pyramidal arrangement. ^b Highest possible point symmetry. ^c Subgroups. Solid lines indicate correlations involving proposed site symmetry for the ordered model; dashed lines, other correlations.

of site symmetries appropriate to an ordered model.

The model in P4 consists of the coaxial arrangement of InCl₅²⁻ and (C₂H₅)₄N⁺ ions situated about the Wyckoff g positions of C₂ symmetry. The In, apical Cl, and N atoms are constrained to the twofold axes with z coordinates identical with those in P4/n. As input to a refinement in P4, positions for the basal Cl atoms were obtained directly from the solution in P4/n.²¹ Coordinates for the C atoms of the coaxial cations were generated from the disordered solution by selecting those atomic positions which correspond to an ordered (C₂N₅)₄N⁺ ion with a twofold axis. The two remaining (C₂H₅)₄N⁺ ions in the unit cell are arranged about the Wyckoff b and d positions with the N atoms assigned to the S₄ sites. Ordered C atom positions were obtained by deconvoluting the disordered arrangement so as to yield mirror image (C₂H₅)₄N⁺ ions.

One feature of the diffraction effect which would normally distinguish P4/n from P4 is the glide absent reflections characteristic of P4/n: hk0, h + k ≠ 2n. Atoms which populate the Wyckoff g sites of P4 cannot contribute to the intensity of these characteristic reflections; therefore, a pseudo n-glide condition would be expected in P4 since the In atoms and, to some extent, the apical Cl atoms will dominate the scattering. The situation is, however, considerably more complex because of the similarity of the atomic arrangements in the original and present models. The characteristic re-

flexions gain intensity only insofar as (1) the InCl_5^{2-} ion deviates from C_4 symmetry, (2) the C atoms of the $(\text{C}_2\text{H}_5)_4\text{N}^+$ ions at the g sites deviate from S_4 symmetry, and (3) the C atoms of the $(\text{C}_2\text{H}_5)_4\text{N}^+$ ions at the b and d sites deviate from a mirror-image relationship.

Three approaches were taken to distinguish the published centrosymmetric model from the present one which lacks a center of symmetry: (1) the performance of tests for a center of symmetry in the crystals; (2) a careful search on the diffractometer for the characteristic reflections ($hk0$, $h+k \neq 2n$); (3) a refinement in $P\bar{4}$ to confirm the viability of the model and to ascertain what structural differences appear during the course of the refinement.

Evidence for a Noncentrosymmetric Space Group. Crystals of $[(\text{C}_2\text{H}_5)_4\text{N}]_2[\text{InCl}_5]$ and $[(\text{C}_2\text{H}_5)_4\text{N}]_2[\text{TlCl}_5]$ were tested for both piezoelectricity and second harmonic generation (SHG). The piezoelectric tests, performed on a Giebe-Schiebe apparatus, were negative for both materials and thus provide no definitive information concerning the absence of a center of symmetry in the crystals.

The SHG tests on index-matched powdered samples of the In and Tl salts showed a weak acentricity. The signal level was $1/3000$ th of the $\alpha\text{-SiO}_2$ standard. However SHG signal from the materials used in preparing the crystals showed that 1 part in 1000 of the noncentrosymmetric compound $[(\text{C}_2\text{H}_5)_4\text{N}][\text{InCl}_4]$ could produce the same signal as that observed for the pentachloride. Simultaneous measurement of the linear scattering and SHG on mixtures of the pentachlorides in several index oils demonstrated that the SHG signal intensities were strongest when the powdered crystallites were appropriately index matched.

The Search of the $hk0$ Zone. A careful search for the characteristic reflections in the $hk0$ zone was carried out on the diffractometer. The 97 data were processed as described previously^{17,23} yielding 49 reflections with $h+k=2n$ and 48 reflections with $h+k \neq 2n$. The value of p used in the estimation of $\sigma(F_o^2)$ was 0.04. The diffraction profiles were carefully examined for spurious effects and one reflection (100) was eliminated because it occurred in a region of high background intensity. Of the 47 characteristic reflections ($h+k \neq 2n$), all except one had $-2.0 \leq F_o^2/\sigma(F_o^2) \leq +2.0$. The 830 reflection had $F_o^2/\sigma(F_o^2) = 3.0$. Assuming that the space group is Pn/n , the probability of such an occurrence is only 0.27%.²⁴ This result is consistent with the noncentrosymmetric structure which was indicated by the second harmonic generation results.

The Refinement in $P\bar{4}$. Full-matrix least-squares refinement²⁵ of the model proceeded satisfactorily, based on the reported 813 observed reflections.² The function minimized was $\sum w(|F_o| - |F_c|)^2$. A scheme similar to that used in the previous reported structure² was employed to assign individual weights, w , to each reflection. The neutral atom scattering factors for In, Cl, N, and C were obtained from the usual tabulation.²⁶ The anomalous terms for In and Cl were obtained from the tabulation of Cromer and Liberman²⁷ and included in F_c .²⁸ Several cycles of least-squares refinement of an isotropic thermal model led to values of 0.095 for R_1 and 0.151 for R_2 . The discrepancy indices, R_1 and R_2 , are defined as $\sum \|F_o| - |F_c|\| / \sum |F_o|$ and $(\sum w(|F_o| - |F_c|)^2 / \sum w F_o^2)^{1/2}$, respectively. The value of R_1 for the isotropic refinement in $P\bar{4}$, 0.095, may be compared with the corresponding value from the refinement in $P4/n$, 0.095.² A difference Fourier map based on the isotropic refinement in $P\bar{4}$ showed no significant residual electron density in the region of the basal Cl atoms. The refinement was then expanded to include an anisotropic thermal model for all atoms. However, it was not possible to refine the N atoms in this manner because of high correlations between various components of the anisotropic tensors.²⁹ The

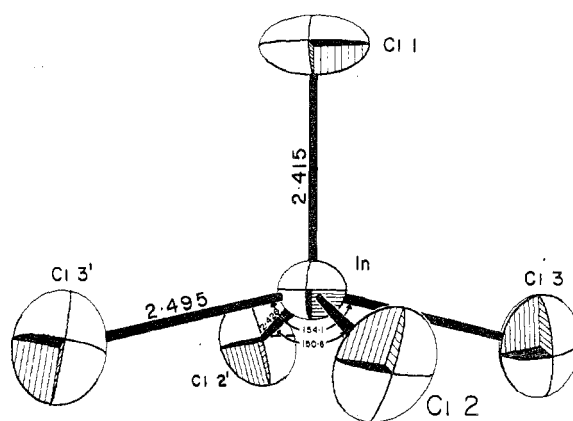


Figure 3. Drawing of the InCl_5^{2-} ion, as determined from a refinement in the $P\bar{4}$ space group. The 50% probability contours are shown. Errors in the last digit(s) of the bond distances are ± 6 , 9, and 11 Å for InCl_1 through InCl_3 , respectively. Standard errors in the bond angles are $\pm 5^\circ$ for $\text{Cl}_2\text{-In-Cl}_2'$ and $\pm 6^\circ$ for $\text{Cl}_3\text{-In-Cl}_3'$.

thermal coefficients of these three atoms were returned to the isotropic form and the refinement was continued leading to final values for R_1 and R_2 of 0.067 and 0.111. A difference Fourier map based on this refinement revealed chemically reasonable positions for 12 of the 20 independent H atoms. The highest nonhydrogen peak on the map was $0.7 \text{ e}/\text{\AA}^3$. This value is approximately one-fifth the height of a typical C atom in the structure.

A structure factor calculation for the $hk0$ zone based on the refined positions in $P\bar{4}$ revealed 13 characteristic reflections with $F_{o,\text{min}} \leq F_c \leq 2F_{o,\text{min}}$. However, it was thought that their calculated intensity might arise indirectly from the fact that the characteristic reflections were not included in the refinement. The data for the $hk0$ zone were therefore merged with the hkl ($l \neq 0$) data of Brown, Einstein, and Tuck via a scale factor obtained from the standard reflections used to monitor crystal stability during data collection. The characteristic reflections in the $hk0$ zone which had $F_o^2 < 1.0$ ($\sim 50\%$) were arbitrarily assigned values of $F^2 = 1.0$. Individual weights for the $hk0$ reflections were taken as $4F_o^2/\sigma^2(F_o^2)$ while the weights for the remaining reflections were taken as described above. An additional cycle of least-squares refinement of the model based on the merged data set resulted in values of 0.079 and 0.092 for R_1 and R_2 , respectively, and did not significantly affect the positional parameters for the InCl_5^{2-} ion, but the number of characteristic reflections with $F_c > F_{o,\text{min}}$ had decreased to 3.

The parameters obtained from the final cycle of anisotropic refinement employing the unmerged data are presented as supplementary data in the microfilm edition along with their estimated standard deviations as obtained from the inverse matrix. A selection of bond distances and angles will be found in Figure 3, and a more detailed tabulation may be found in the microfilm edition. The structure of $[(\text{C}_2\text{H}_5)_4\text{N}]_2[\text{InCl}_5]$ as refined in $P\bar{4}$ is, as expected, very similar to the model in $P4/n$. Because of this similarity, the general description of the structural features, as provided by Brown, Einstein, and Tuck,² and most of the conclusions drawn therefrom are adequate for the model in $P\bar{4}$.

During the refinement in $P\bar{4}$, small but significant changes occur in the basal plane of the InCl_5^{2-} ion. The basal Cl atoms have moved by $\sim 0.5 \text{ \AA}$ from their fourfold symmetric positions in $P4/n$, leading to variations in the bond distances and angles about the In atom (Figure 3) that are qualitatively sufficient to explain the vibrational results.

Conclusions

The new single-crystal and low-temperature Raman spectra

demonstrate that the effective symmetry of MX₅²⁻ species in [(C₂H₅)₄N]₂[InCl₅] is lower than the C₄ site symmetry which was assigned in the original structure determination. This reinterpretation of the vibrational data provides a ready explanation of the anomalous E symmetry mode which plagued earlier vibrational studies of the pentachloroindate salt.

The distorted InCl₅²⁻ unit could be accommodated by postulation disorder of the complex about a C₄ axis in the original space group P4/n or by a new space group assignment. We favor the latter interpretation because X-ray and second harmonic generation experiments indicate that [(C₂H₅)₄N]₂[InCl₅] and [(C₂H₅)₄N]₂[TiCl₅] may crystallize in a noncentrosymmetric space group. Refinement of the published X-ray data in the logical noncentrosymmetric space group, P4̄, leads to a small C₂ distortion of the InCl₅²⁻ complex, with two of the basal chlorines slightly displaced toward the axial positions of a trigonal bipyramid and the remaining two slightly displaced toward the equatorial positions (Figure 3). Unlike the original structural determination, the present refinement does not require disorder of the cations. Two other pleasing improvements are the lack of large residuals around the InCl₄ equatorial plane in the electron density map and the location of most of the hydrogen atoms associated with the cation. Thus, details of the structural reinterpretation are quite reasonable and are consistent with the vibrational data.

An X-ray space group determination along with detailed single-crystal Raman spectra and second harmonic generation experiments demonstrate that [(C₂H₅)₄N]₂[TiCl₅] is isostructural and isostructural with the indium salt. In particular the vibrational data again indicate a C₂ distortion of a square-pyramidal TiCl₅²⁻ ion. This result affords detailed confirmation of the postulated similarity in structure of the indium and thallium complexes.⁵

Aside from their significance in elucidating the structures, the vibrational data are of interest for possible clues as to why these complexes, which contain no lone electron pairs on the central metals, should adopt a square-pyramidal structure rather than the expected trigonal bipyramid. It was previously pointed out that the normal mode which could lead to a square pyramid → trigonal bipyramid interconversion has an unusually high frequency when compared with other deformation modes.⁸ By contrast, this is one of the lowest frequency modes for square-pyramidal species containing a lone pair on the central atom.^{8,30} This comparison still remains valid with the new assignments.³¹ Another indication of the rigidity of InCl₅²⁻ and TiCl₅²⁻ is the similarity in ordering between the deformation modes for these complexes and those of octahedral stereochemically rigid MX₅L complexes.³¹ The most obvious origin of the rigidity of pentachloroindate and -thallate is cation-anion contacts in the solid. In harmony with this idea, the C₂ distortion of the InCl₅²⁻ complex conforms to the spatial requirements of the α-carbon atoms of the coaxial (C₂H₅)₄N⁺ ions.

Acknowledgment. We appreciate the advice and access to X-ray equipment provided by Professors J. A. Ibers and J. B. Cohen. A. P. Gaughan acknowledges the receipt of a NIH postdoctoral fellowship. This work was supported by the Advanced Projects Agency through the Northwestern Materials Research Center.

Registry No. [(C₂H₅)₄N]₂[TiCl₅], 55399-18-3; [(C₂H₅)₄N]₂[InCl₅], 34978-51-3.

Supplementary Material Available. A listing of positional and thermal parameters and a detailed tabulation of bond distances and angles appear following these pages in the microfilm edition of this volume of the journal. Photocopies of the supplementary material from this paper only or microfiche (105 × 148 mm, 24× reduction, negatives) containing all of the supplementary material for the papers in this issue may be obtained from the Journals Department, American Chemical Society, 1155 16th St., N.W., Washington, D.C. 20036. Remit check or money order for \$4.00 for photocopy or \$2.50 for microfiche, referring to code number AIC502063.

References and Notes

- (1) A. L. Beauchamp, M. J. Bennett, and F. A. Cotton, *J. Am. Chem. Soc.*, **90**, 1718 (1968).
- (2) D. S. Brown, F. W. B. Einstein, and D. G. Tuck, *Inorg. Chem.*, **8** 14 (1969).
- (3) R. R. Holmes, *Acc. Chem. Res.*, **5**, 296 (1972).
- (4) I. Wharf and D. F. Shriver, *Chem. Commun.*, 528 (1968).
- (5) D. F. Shriver and I. Wharf, *Inorg. Chem.*, **8**, 2167 (1969).
- (6) J. Gislason, M. H. Loyd, and D. G. Tuck, *Inorg. Chem.*, **10**, 1907 (1971).
- (7) J. G. Contreas, J. S. Poland, and D. G. Tuck, *J. Chem. Soc., Dalton Trans.*, 922 (1973).
- (8) S. R. Leone, B. Swanson, and D. F. Shriver, *Inorg. Chem.*, **9**, 2189 (1970).
- (9) D. M. Adams and R. R. Smardzewski, *J. Chem. Soc. A*, 714 (1971).
- (10) J. G. Contreas and D. G. Tuck, *Inorg. Chem.*, **11**, 2967 (1972).
- (11) D. F. Shriver, R. Loyd, and W. Davis, XXIIth Mid-America Symposium on Spectroscopy Final Program, Chicago, Ill., 1970, p 46; G. C. Joy, III, Ph.D. Thesis, Northwestern University, 1974.
- (12) J. Pitha and R. W. Jones, *NRC Bull.*, No. 12, 9 (1968).
- (13) S. K. Kurtz and T. T. Perry, *J. Appl. Phys.*, **39**, 3798 (1968).
- (14) S. C. Abrahams, *J. Appl. Crystallogr.*, **5**, 143 (1972).
- (15) J. P. Dougherty and S. K. Kurtz, Abstracts, American Crystallographic Association Meeting, March 1974, Paper N1.
- (16) S. K. Kurtz and J. P. Dougherty, "Systematic Materials Analysis", Vol. IV, Academic Press, New York, N.Y., in press.
- (17) P. W. R. Corfield, R. J. Doedens, and J. A. Ibers, *Inorg. Chem.*, **6**, 197 (1967).
- (18) P. K. Narayanaswami, *Proc. Indian Acad. Sci., Sect. A*, **26**, 521 (1947).
- (19) Selection rules for the original C_{4h} unit cell require 9 modes in the Raman: 3 A_g, 3 B_g, and 3 E_g. With negligible factor group coupling these will coincide with 3 A_u, 3 B_u, and 3 E_u infrared-active counterparts. If, however, it is assumed that the MX₅²⁻ ions reside in sites of local C₂ symmetry (which are disordered to produce an apparent C₄ axis in the X-ray diffraction), 12 Raman-active crystal modes will result under conditions of negligible factor group coupling.
- (20) (a) J. T. Mague, *Inorg. Chem.*, **8**, 1975 (1969); (b) D. W. Cruickshank and J. S. Rollett, *Acta Crystallogr.*, **6**, 705 (1953); **9**, 203 (1956).
- (21) Atomic positions derived from the solution in P4/n must be adjusted for the different origins in the two space groups.
- (22) S. K. Kurtz, Ninth International Congress of Crystallography, Kyoto, Japan, Sept 1972, Paper XXIIIa-5, Abstract P, S-231.
- (23) R. J. Doedens and J. A. Ibers, *Inorg. Chem.*, **6**, 204 (1967).
- (24) R. C. Weast, Ed., "Handbook of Chemistry and Physics", 48th ed, Chemical Rubber Publishing Co., Cleveland, Ohio, 1967, p A157.
- (25) In addition to various local programs for the CDC 6400 computer, modified versions of the following programs were employed: Zalkin's FORDAF Fourier summation program, Johnson's ORTEP thermal ellipsoid plotting program, Busing and Levy's ORFFE error function program, and the full-matrix least-squares program NUCL5.
- (26) D. T. Cromer and J. T. Waber, "International Tables for X-Ray Crystallography", Vol. IV, Kynoch Press, Birmingham, England, 1974, Table 2.2A.
- (27) D. T. Cromer and D. Liberman, *J. Chem. Phys.*, **53**, 1891 (1970).
- (28) J. A. Ibers and W. C. Hamilton, *Acta Crystallogr.*, **17**, 781 (1964).
- (29) Specifically, β₁₁ and β₃₃ of N₂ (1/2, 1/2, 1/2) are highly correlated with β₁₁ and β₃₃ of N₃ (0, 0, 1/2), respectively, because of the pseudo center of symmetry at 1/4, 1/4, 1/2. In addition, β₁₁ and β₂₂ of N₁ are highly correlated because of the pseudo-fourfold symmetry about the crystallographic twofold axes.
- (30) L. F. Drullinger and J. E. Griffiths, *Spectrochim. Acta, Part A*, **27**, 1793 (1971).
- (31) D. M. Byler and D. F. Shriver, *Inorg. Chem.*, **13**, 2697 (1974).